

An Automatic Weight-Based High Dynamic Range Imaging Syntheses with Multiple Different Exposed Low Dynamic Range Images

¹Jiun-You Chen and ²Chen-Chung Liu

Abstract

High dynamic range (HDR) imaging offers the capture of faithful representations of real world scenes to become a powerful technique in many areas, providing the maximum amount of detail data for radiologists to examine medical MR images. Now, HDR imaging is widely utilized in surveillance, remote sensing, and space research. This paper proposes a simple and effective scheme to generate a single HDR image combined by multiple low dynamic range (LDR) images of a scene with different exposures. The proposed algorithm first divides each LDR image into non-overlapping blocks of the same size, and then evaluate each block's average intensity and the statistical values of intensities of the whole LDR images. The proposed approach gives weight for each block according to each block's average intensity. The final output block is assigned as a weighted average of the input blocks acquired at different exposures. The experimental results show that the proposed approach has three major advantages: (i) the proposed algorithm is simple and effective, (ii) the proposed algorithm is time saving, due to operating completely on intensity only, (iii) there are no restrictions in the image dynamic color ranges in the proposed algorithm.

Keywords : High dynamic range (HDR), low dynamic range (LDR), weight.

*Corresponding Author: Jiun-You Chen
(E-mail: gn00139173@yahoo.com.tw)

¹Taipei College of Maritime Technology, Tamsui, New Taipei, Taiwan

²Department of Electronic Engineering, National Chin-Yi University of Technology

The work was partially supported by the National Chin-Yi University of Technology, Taiwan, under research contract NCUT 14-R-CL-013.

1. Introduction

In science, the dynamic range is defined as a ratio of the maximum physical measure to the minimum physical measure. In photography, the definition of dynamic range depends on what the dynamic range refers to. The dynamic of scenes is the brightness ratio of the brightest part to the darkest part, and the dynamic of displays is the ratio of the maximum luminance to the minimum luminance emitted from the screen, and the dynamic of images is the brightness ratio of the brightest part to the darkest part of the image [1, 2, 3]. An image or a scene is defined to be high dynamic range (HDR) while its dynamic range extremely exceeds the dynamic range of the capture or display devices. Real-world scenes are often HDR because they can always contain a very enormous range of light intensities at the same time. For instance, in a sunny day we want to take a photograph that contains the inside of a room and some exterior scenes visible through windows. In most cases, the exterior scenes will be very bright due to the sun's directly illuminating, while the illumination of the inside of the room is far darker. In order to make features in the dark areas visible, one may use higher exposure to acquire an image, which displays appropriately exposed details in the room and renders the bright area saturated to lose all details of the exterior scene. On the other hand, one may utilize lower exposure to properly expose the exterior scenes to make features in the exterior scenes visible, but the interior of the room will be underexposed so to lose all details of the room [4, 5, 6].

In fact, traditional low range dynamic (LRD) imaging cannot completely display all the detail features of a scene that are detected by human visual system. On the other hand, with the rapid progressions in computer graphing and digital imaging technologies, people have been increasing interests in high dynamic range (HDR) imaging [7, 8]. HDR imaging offers the capture of faithful representations of real world scenes, so it becomes a powerful technique in many areas; in medical imaging, it provides the maximum amount of detail data for radiologists to examine medical MR images. In digital photography, it produces preferred pictorial images, faithfully reproduces overall appearance of original scenes and the contrast relationships between objects in the scene, and predicts the visibility of specific objects in a scene [9, 10]. Now, HDR imaging is widely utilized in surveillance, remote sensing, and space research. Many researches have shown that HDR imaging has much better performances than that of LDR imaging in these areas mentioned above.

The main purpose of high dynamic range imaging is to accurately represent the real world scenes with a large range of brightness from the brightest sunlight to the darkest shadow. Now, there are many methods to obtain the so-called high dynamic range (HDR) images : (i) created directly with Computer-generated images ; (ii) obtaining from modern imaging-hardware; advanced HDR-CCD digital cameras are combined with two different exposure CCDs so they can get the HDR that is four times of the traditional camera's HDR ; (iii) generating by combining the information from multiple LDR images taken at different exposure settings [11, 12, 13]. The third method is the most popular and most effective, it detects saturated pixels in the images and compensates these saturated pixels with the pixels of the images taken under other exposure conditions. People can easily set the optimal exposure conditions to improve dynamic range through exposure time control because the exposure time can be controlled accurately.

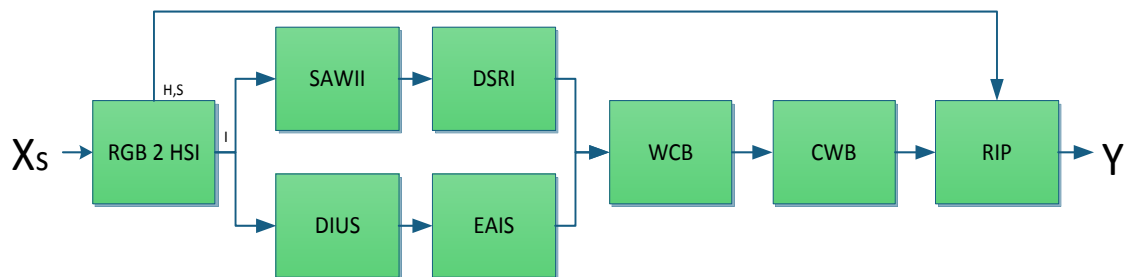
The most popular method to generate HDR images is to sequentially take multiple images of the scene using different exposures. High exposures provide useful information in dark scene regions, yet low exposures offer useful information in dark scene regions. Therefore, these different exposed images can be fused to get a single HDR image. To acquire HDR images from combining multiple LDR images was first reported by Mann & Picard [14]. They examined the situation of each different exposure images of a scene to give weight for each image, and these weighted images are merged to form a single HDR image. Debevec and Malik [15] utilized multiple exposures to increase the dynamic range of images. They gave higher weight to input pixels whose intensities are nearer to the mean of all the pixels of input images, and less weight to the input pixels whose intensities are more far away from the mean of all the pixels of input images. The final output pixels are specified as a weighted average of the input pixels acquired at different exposures. Chen and Mu [16] proposed an interactive cut-and-paste scheme to increase images' dynamic ranges, where blocks of the resultant image are manually selected from blocks of the input images. Additional works about HDR imaging have been done by Mitsunaga & Nayar [17], Robertson et al.[18], and Robertson et al [19]. We propose a simple and effective scheme to generate a single HDR image combined by multiple LDR images with different exposures of a scene; the method is an extension to merge Chen et al method and Debevec et al method. Our scheme does not need to estimate the response function of the image capture device. We first divide each LDR images into non overlapping blocks of the same size, and then evaluate each block's average intensity and the statistical values of intensities of the whole LDR images. Our algorithm gives higher weight to blocks whose average intensities are nearer to the mean of all the corresponding blocks that are at the same place in the result image, and less weight to blocks whose average intensities are nearer to the mean of all the corresponding blocks that are at the same place in the result image. The final output block is assigned as a weighted average of the input blocks acquired at different exposures. The experimental

results show that the proposed algorithm is effective and valid. The remainder of this paper is organized as follows; Section 2 presents the proposed algorithm. Section 3 describes the empirical results. Section 4 concludes this paper.

2. Proposed Object Extraction Algorithm

An efficient high dynamic range imaging scheme for color images must be precise and time-saving. In order to construct a superior high dynamic range imaging algorithm for LDR color images, several schemes are used in this paper to achieve the goal. The overall process of the proposed high dynamic range imaging scheme for color images is shown in Figure 1. The input RGB color images of a scene with different exposures are transformed into

HSI color space. The proposed scheme first divide each intensity plane of HSI images into non overlapping blocks with the same size, and then evaluate each block's average intensity and the statistical values of intensities of the whole HSI images. Our algorithm give higher weight to blocks whose average intensities are nearer to the mean of all the corresponding blocks that are at the same place in the result image, and less weight to blocks whose average intensities are nearer to the mean of all the corresponding blocks that are at the same place in the result image. The final output block is assigned as a weighted average of the input blocks acquired at different exposures. Some basic theory about human visible system, the brightness of a scene, and steps of the proposed algorithm are described in detail in the following subsections.



X_s : different-exposed low dynamic range images of a scene
 SAWII : statistical analysis of whole images' intensities
 DIPB : dividing Intensity plane into unoverlapped sub blocks
 EAIB : evaluating the average intensity of sub blocks
 RGB2HSI : color space transformation from RGB domain to HIS domain

Y : output the result high dynamic rang image
 WCB : weight eaculation of each sub blocks
 CWB : combination of weighted sub blocks
 DSRI : determining the suitable range of intensity
 RIP : resultant intensity plane

Figure 1: The flow chart of the proposed high dynamic range imaging scheme.

2.1 Human Visual System and Scene Brightness

The human visual system (HVS) can perceive about 4 orders of magnitude of light intensities at any one moment. The HVS can also be adjusted another 6 orders up and down through its own adaptation process. This adaptation process of HVS does not work instantaneously and may take several minutes, for example, in the case of entering a dark place from a bright environment [8]. Even though the HVS can cover that huge range of light intensities, it does not mean that people can see equally well at all intensity levels, since the HVS has two kinds of

photoreceptors, rods and cones, which have different sensitivities, respectively. Rods can detect small luminance differences in low-light-environments, but their ability for distinguishing colors is poor due to their visual sharpness. It is named scotopic vision. On the other hand, the three types of cones are conscientious for distinguishing a sharp vision of colors under well lightness conditions. This is called photopic vision. Moreover, the overlapping region of the scotopic and photopic ranges is called mesopic. The cones have an obstacle in distinguishing luminance levels, which have to be large enough to be detectible [10]. These

differences of detectible light intensities were evaluated in psychophysical studies. They have illustrated that over a large range of light intensity, the minimum detectible light difference is almost constant around 1% [2]. The minimum detectible light difference is called the visible threshold or just-noticeable difference. Furthermore, researchers have shown that the HVS follows a logarithmic function to response to light intensities.

The observed brightness of a scene is referred as luminance, measured in candela (cd) per square meters [2]. For example, the surface of the sun has an intensity about 2×10^9 cd/m², a moonless night sky has a luminance level about 3×10^{-5} cd/m², and a daylight scene is close to 10^5 cd/m² [4]. The dynamic range of brightness (radiance) values approximates $10^6:1$ for a typical real-world scene, $10^{12}:1$ for human eyes after adapting, up to $8 \times 10^3:1$ for camera sensor, and less than $10^3:1$ for monitor. Although the HVS has a dynamic range of brightness approximately twelve orders of magnitude to distinguish huge range of light intensities in the real world scene. But the current performance of modern digital image capture and display devices still suffer from a limited dynamic range. These devices are called low dynamic range (LDR) reproduction devices in this paper. Digital cameras utilized in computer vision usually offer 8 bits of brightness information for each color channel at each pixel. For each color channel, all radiance intensities in the scene are mapped to one of 256 image brightness levels. Computer vision problems, such as the shape detection of objects, the motion estimation of objects, and the recognition of objects, are often under-controlled and thus essentially hard to be solved. The low dynamic images produced by today's low dynamic range reproduction devices make dark areas darker and make bright areas brighter, losing more features to cause each of these problems more difficult.

2.2 Color Model Transformation from RGB to HSI

For measuring or reproducing color, a number of three dimensional color models are defined, among which the most popularly used is RGB (Red, Green, and Blue) model [20]. The RGB model is a physical system, and the image in the RGB model is the most suitable for color image representation. However, it is not suitable for image processing applications because its R, G, and B components are highly correlated. The distance in the RGB color space does not stand for the perceptual difference in a uniform scale. In image processing and analysis, these R, G, and B components are often transformed into other color models. Modern techniques for HDR imaging are basically developed on the RGB color space. Luminance-chrominance color space representations are frequently neglected. On the other hand, employing HDR imaging techniques in luminance-chrominance space may be better for the following reasons: (i) The intensity channel of Luminance-chrominance color space is the weighted average of the R, G, and B channels. It has a higher signal-to-noise ratio (SNR). (ii) Luminance-chrominance color space is a decorrelated color space so to offer better compressibility. Therefore, most part of image compression techniques store images in Luminance-chrominance color space. While one utilizes the already-compressed multiple-exposure LDR images to make a HDR image, it is more efficient and time saving to generate the HDR image, because the final HDR image is more suited for compression and display. (iii) HDR techniques working in RGB space always need post-composition white balancing. The white balancing should create perceptually convincing colors which may not be the true colors. In this paper, we address the HDR imaging in HIS color space to improve the performance of HDR imaging [21].

The HSI (Hue, Saturation, and Intensity) color model is the most representative of the perceptual systems, which is widely used in image processing. The advantages of the HSI model are: hue and saturation have good correlation with the human perception of colors and its separability of chromatic values from achromatic values. The HSI reduces the redundancy models in the RGB model, and its components H (hue), I (intensity), and S (saturation) are given using some color transform from the RGB color space [22].

$$H = \begin{cases} \theta & \text{if } B \leq G \\ 360 - \theta & \text{if } B > G \end{cases} \quad (1)$$

$$\theta = \cos^{-1} \left\{ \frac{\frac{1}{2}[(R-G) + (R-B)]}{\left[\frac{1}{4}[(R-G)^2 + (R-B)(G-B)] \right]^{1/2}} \right\} \quad (2)$$

$$S = 1 - \frac{3}{(R+G+B)} [\min(R, G, B)] \quad (3)$$

$$I = \frac{1}{3}(R+G+B) \quad (4)$$

In the HSI color model the saturation corresponds to the relative purity of a color. The hue stands for the dominant wavelength in mixed light and indicates a dominant color as perceived by the human eyes. The intensity or perceived lightness indicates the brightness of a color.

2.3 HDR Image Synthesis

Since the hue and saturation planes of different exposure images of a scene are the same, the proposed algorithm does not change the hue and saturation planes to maintain their original colors. For estimating the combination weight of each intensity plane, the mean and standard deviation of intensity of the set of different exposure images of a scene are evaluated by the following equations:

$$\mu_i = \sum_{x=1}^W \sum_{y=1}^H I_i(x, y) / (W \times H), \quad (5)$$

$$\mu = \sum_{i=1}^N \mu_i / N, \quad (6)$$

$$\sigma = \sqrt{\sum_{i=1}^N \sum_{x=1}^W \sum_{y=1}^H (I_i(x, y) - \mu)^2 / (N \times W \times H)}, \quad (7)$$

where $I_i(x, y)$ is the intensity of pixel $p_i(x, y)$ in the image i , W is the width and H is the height of the input image, and N is the number of images set of N different exposure images of a scene. The proposed algorithm divides each intensity plane into non overlapping blocks with the same size $m \times n$, evaluates each block's average intensity, and then determines each block's combination weight using following equations.

$$v_i(j, k) = \sum_{x=j \times m}^{j \times m + m - 1} \sum_{y=k \times n}^{k \times n + n - 1} I_i(x, y) / (m \times n), \quad (8)$$

$$j = 0, 1, 2, \dots, [W/m], k = 0, 1, \dots, [H/n],$$

$$\omega_i(j, k) = \exp(-(v_i(j, k) - \alpha\mu)^2 / \sigma^2) / \sum_{i=1}^N \exp(-(v_i(j, k) - \alpha\mu)^2 / \sigma^2), \quad (9)$$

where $v_i(j, k)$ is the average intensity of block (j, k) of image i , $\omega_i(j, k)$ is the combination weight of block (j, k) of image i , and α is the adjustment coefficient with value between 0.1 and 1. The intensity of a block of the result HDR image is the weighted sum of intensities of corresponding blocks located at the same place, and the intensity plane of the resultant HDR image is the composition of these result intensity blocks.

3. Experiment Result

This section presents experimental results under various conditions to illustrate the utility and efficiency of the proposed scheme. Experiments in this paper are conducted on a computer with a 2.8GHz Intel Pentium processor and 2 GB RAM running Matlab version 7.6, and the input RGB color images are 2048×1360×3 pixels.

Figure 2 shows a high dynamic range imaging example with the proposed adaptive weighted sum (AWS) algorithm for a static window scene. Row 1 shows five input LDR images of a static window scene taken at different exposure times from brightest to darkest, i.e. 1/13, 1/25, 1/50, 1/100, and 1/200 seconds by using a Nikon D5100 digital camera with aperture f/8. Row 2 shows five corresponding output HDR images of these input window scene images generated at different adjustment coefficients from left to right, i.e. 0.2, 0.4,

0.6, 0.8, and 1. Row 2 shows that both indoor and outdoor scenes are clearer while the different adjustment coefficient is decreasing, so that more detail features can be detected. Row 3 shows four corresponding output HDR images of the red-swath image of (c1) while generated with different block size from (c2) to (c5), i.e. 3×3, 4×4, 6×6, and 8×8 pixels. Row 3 shows that the visible quality of the result HDR image largely depends on the block size, the edges of objects in the HDR image is smoother while the size of blocks is decreasing.

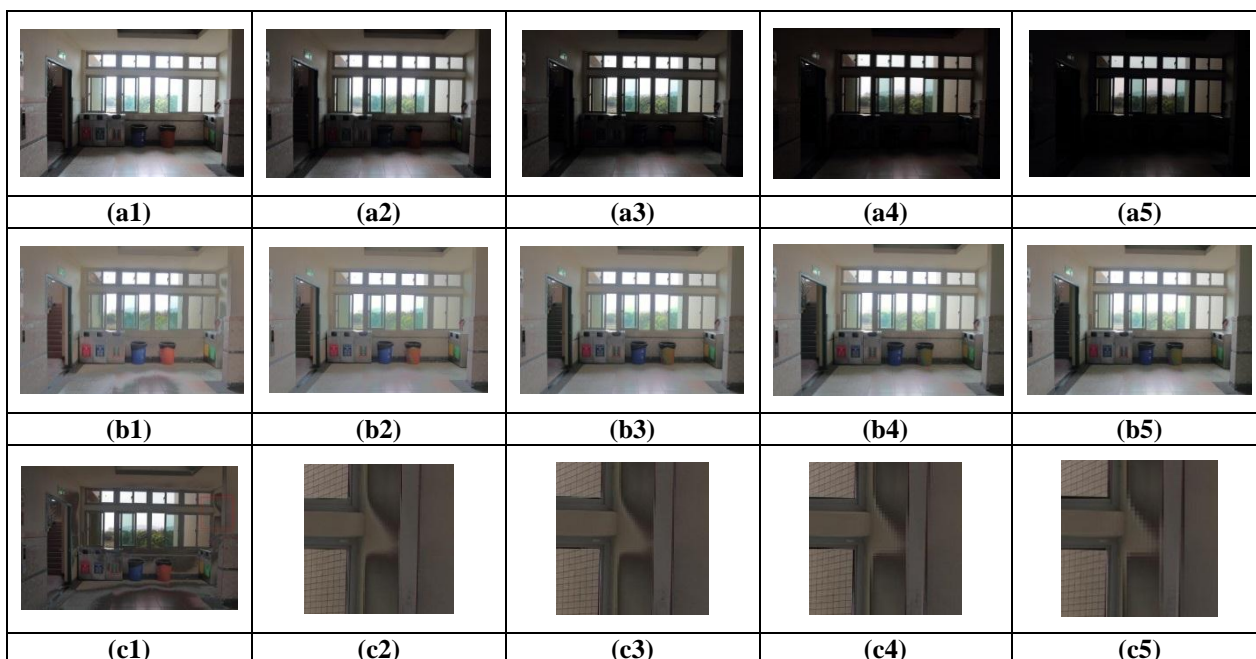


Figure 2: A HDRI example of the proposed AWS algorithm for a static window scene

Table 1 shows the time consumption of the proposed AWS algorithm applied on varying block sizes and varying number of input images. Table 1 shows that the time consumption is increasing while

the number of blocks is increasing. Moreover, the time consumption is increasing little while the number of blocks is increasing.

Table1: Time consumption (in seconds) of the proposed AWS algorithm vs. block sizes and the number of input images

Block size images	3×3	4×4	5×5	6×6	7×7	8×8
3	101.5168	58.99292	38.75628	27.29112	20.95876	16.87773
4	123.1983	73.45537	47.77556	34.38825	26.75953	21.16526
5	149.8255	86.68965	58.79428	42.58425	31.89567	25.66855

Figure 3 shows another high dynamic range imaging example with the proposed adaptive weighted sum (AWS) algorithm for a static scene; (a1) shows the input over-exposure image with exposure value negative one, (b1) shows the input suitable exposure image with exposure value zero; (c1) shows the input under-exposure image with exposure value positive one; (d1) shows the image of hue plane of input image; (d2) shows the image of the saturation plane of input image; (a2) is the image of intensity plane of (a1); (b2) is the image of intensity plane of (b1); (c2) is the image of intensity plane of (c1); (a3) is the image of weighted intensity plane of (a1); (b3) is the image of weighted intensity plane of (b1); (c3) is the image of weighted intensity plane of (c1); (d3) is the image of sum of weighted intensity planes of input images; (d4) is the result HDR image generated

by the proposed AWS algorithm; (a4) is the image of the absolute difference between the result HDR image and the input over-exposure image; (b4) is the image of the absolute difference between the result HDR image and the input suitable-exposure image; (c4) is the image of the absolute difference between the result HDR image and the input under-exposure image.

Figure 3 show that not only the visible regions are preserved, but also the overexposed and underexposed areas in the original LDR images are modified suitably in the result HDR image. These facts show that the proposed algorithm can transform the source image's colors to the target image effectively and accurately.

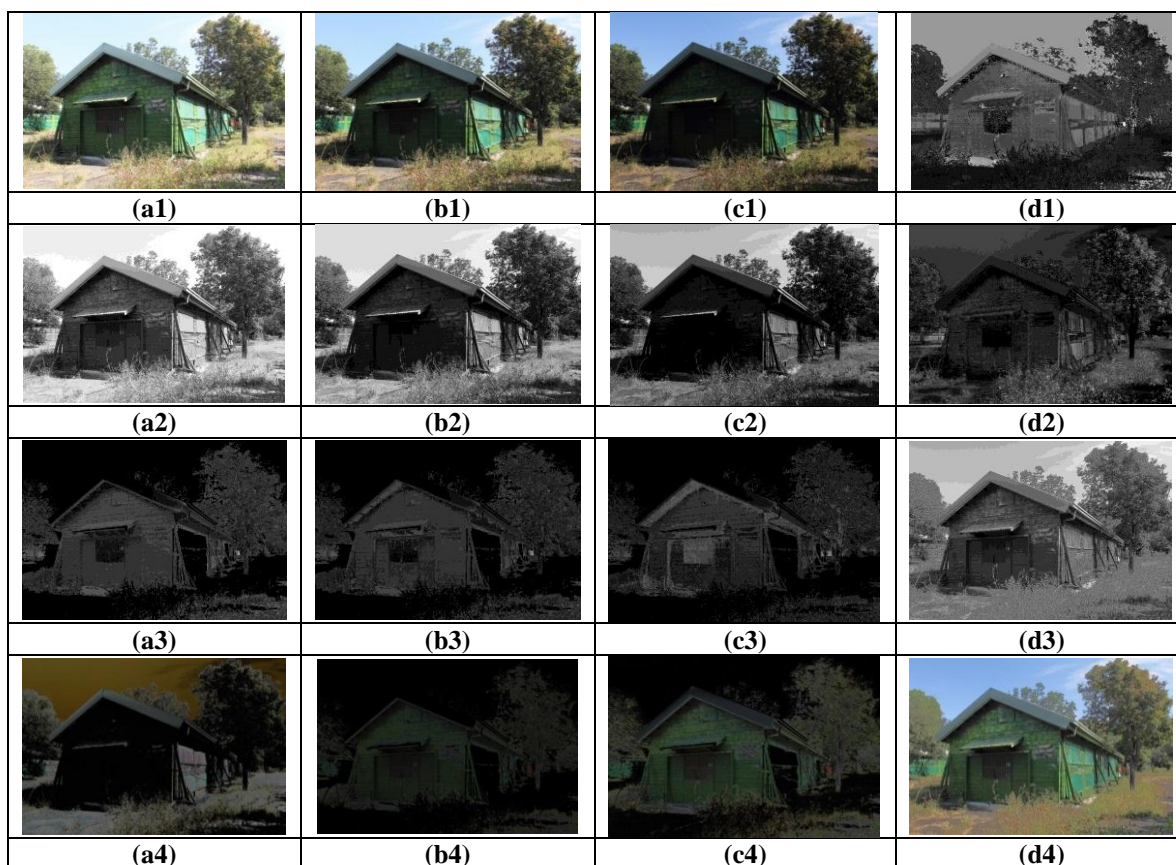


Figure 3: A high dynamic range imaging example using the proposed adaptive weighted sum (AWS) algorithm for a static scene.

4. Conclusions

HDR imaging offers the capture of faithful representations of real world scenes to become a powerful technique in many areas, so that it provides the maximum amount of detail data for radiologists to examine medical MR images. Now, HDR imaging is widely utilized in surveillance, remote sensing, and space research. This paper proposes a simple and effective scheme to generate a single HDR image combined by multiple LDR images of a scene with different exposures. The proposed algorithm first divides each LDR images into non overlapping blocks of the same size, and then evaluates each block's average intensity and the statistical values of intensities of the whole LDR images. The proposed algorithm gives weight for each block according to each block's average intensity. The final output block is assigned as a weighted average of the input blocks acquired at different exposures. The experimental results show that the proposed approach has three major advantages: (i) the proposed algorithm is simple and effective, (ii) the proposed algorithm is time saving, due to operating completely on intensity only, (iii) there are no restrictions in the image dynamic color ranges in the proposed algorithm. In the future, we will combine the proposed scheme color transform schemes to improve the qualities of generated HDR images.

References

- [1]. A. Srikantha, D. Sidibe', Ghost detection and removal for high dynamic range images: Recent advances, *Signal Processing: Image Communication*, Vol. 27, pp.650-662, 2012.
- [2]. M. A. Robertson, S. Borman, R. L. Stevenson, Estimation-theoretic approach to dynamic range enhancement using multiple exposures, *Journal of electronic imaging*, Vol. 12, No. 2, pp. 219–228, 2003.
- [3]. S. Silk n, J. Lang, High dynamic range image deghosting by fast approximate background modelling, *Computers & Graphics*, Vol. 36, pp.1060-1071, 2012.
- [4]. L. Meylan, S. Süsstrunk, High Dynamic Range Image Rendering with a Retinex-Based Adaptive Filter, *IEEE Transactions on image processing*, Vol. 15, No. 9, pp.2820-2830, 2006.
- [5]. B. Gu, W. Li, J. Wong, M. Zhu, M. Wang, Gradient field multi-exposure images fusion for high dynamic range image visualization, *J. Vis. Commun. Image R.*, Vol. 23, pp.604-610, 2012.
- [6]. B. Masia, S. Agustin, R. Fleming, O. Sorkine and D. Gutierrez, Evaluation of reverse tone mapping through varying exposure conditions, *ACM Transactions on graphics*, Vol. 28, No.5, 2009.
- [7]. A. Gonçalves, J. P. Moura, L. Magalhães, A. Chalmers, Perceptual images of Conimbriga using High Dynamic Range, *Journal of Archaeological Science*, Vol. 40, pp.116-128, 2013.
- [8]. G. Qiu, J. Duana, G. D. Finlaysonb, Learning to display high dynamic range images, *Pattern recognition*, Vol. 40, pp. 2641 – 2655, 2007.
- [9]. B. Gu, W. J. Li, M. Y. Zhu, M. H. Wang, Local Edge-Preserving Multiscale Decomposition for High Dynamic Range Image Tone Mapping, *IEEE Transactions on Image Processing*, Vol. 22, No. 1, pp. 70–79, 2013.
- [10]. S. Battiato, A. Castorina, M. Mancuso, High dynamic range imaging for digital still camera: an overview, *Journal of electronic imaging*, Vol. 12, No. 3, pp. 459–469, 2003.
- [11]. T. Jinno, M. Okuda, Multiple Exposure Fusion for High Dynamic Range Image Acquisition, *IEEE Transactions on Image Processing*, Vol. 21, No. 1, pp. 358–365, 2012.
- [12]. F. Banterle, K. Debattista, A. Artusi, S. Pattanaik, K. Myszkowski, P. Ledda and A. Chalmers, High dynamic range imaging and low dynamic range expansion for generating HDR content, *Computer graphics forum*, Vol. 28, No. 8, pp. 2343–2367, 2009.
- [13]. M. H. Kim, J. Kautz, Characterization for high dynamic range imaging, *Computer graphics forum (Proc. EUROGRAPHICS 2008)*, Vol. 27, No. 2, pp. 691–697, 2008.
- [14]. S. Mann and R. Picard, Being undigital with digital cameras: Extending dynamic range by combining differently exposed pictures, *IS&T's 48th annual conference*, Cambridge, MA, 1995.
- [15]. P. Debevec and J. Malik, Recovering high dynamic range radiance maps from photographs, *SIGGRAPH 1997: Proceedings of the 24th annual conference on Computer graphics and interactive techniques*, pp. 369–378, 1997.

- [16]. Z. Chen and G. Mu, High-dynamic-range image acquisition and display by multi-intensity imagery, *J. Imaging Sci. Technol.* Vol. 39, No. 6, pp. 559–564, 1995.
- [17]. T. Mitsunaga and S. Nayar, “Radiometric self calibration,” In *Proceedings of IEEE CVPR*, pp. 472–479, 1999.
- [18]. M. A. Robertson, S. Borman, and R. L. Stevenson, “Dynamic range improvement through multiple exposures,” *Int. Conf. Image Process.* 3, 159–163, 1999.
- [19]. M. Robertson, S. Borman, and R. Stevenson, Dynamic range improvements through multiple exposures, *Proceedings of International Conference on Image Processing (ICIP) 1999*, pp. 159–163, 1999.
- [20]. C. Clausen, H. Wechsler, Color Image Compression Using PCA and Back propagation Learning, *Pattern Recognition*, vol.33, pp. 555-1560, 2007.
- [21]. O. Pirinen, A. Foi, A. Gotchev, Color high dynamic range (HDR) imaging: The luminance-chrominance approach, *International journal of imaging systems and technology*, Vol. 17, No. 3, pp. 152-162, 2007.
- [22]. M. Sezgin, B. Sankur, Survey over image thresholding techniques and quantitative performance evaluation, *Journal of Electronic Imaging*, vol. 13, no. 1, pp. 146-165, 2004.



Chen-Chung Liu received the B.S. degree in applied mathematics from National Chung-Hsing University, Taiwan, in 1976, and M.S. degree in physical oceanography from the National Taiwan University, Taiwan, in 1980. He spent two years (82/83) at the National Taiwan Natural Science Museum as an assistant researcher. At present he is a Professor and the head in the Department of Electronic Engineering at National Chin-Yi University of Technology, Taiwan. His research interests include computer graphics, pattern recognition, image analysis, and digital signal processing.



Jiun-You Chen received the B.S. degree in electronic engineering from National Chin-Yi University of Technology, Taiwan, in 2010, and M.S. degree in electronic engineering from National Chin-Yi University of

Technology, Taiwan, in 2012. At present he is a lecture at Taipei College of Maritime Technology, New Taipei, Taiwan. His research interests include computer graphics, 3D model watermarking, pattern recognition, image analysis, and embedded system.